Crossover between liquidlike and gaslike behavior in CH₄ at 400 K

D. Smith,[1,2] M. A. Hakeem,[1] P. Parisiades,[3,4] H. E. Maynard-Casely,[5] D. Foster,[1] D. Eden,[1] D. J. Bull,[1] A. R. L. Marshall,[2]
A. M. Adawi,[2] R. Howie,[6,7] A. Sapelkin,[8] V. V. Brazhkin,[9] and J. E. Proctor[1,2,10,*]

[1]*Materials and Physics Research Group, School of Computing, Science and Engineering, University of Salford,*
Manchester M5 4WT, United Kingdom
[2]*School of Mathematics and Physical Sciences, University of Hull, Hull HU6 7RX, United Kingdom*
[3]*European Synchrotron Radiation Facility, Beamline ID27, Boîte Postale 220, Grenoble, France*
[4]*IMPMC, Université Pierre et Marie Curie, 4 place Jussieu, 75005 Paris, France*
[5]*Australian Nuclear Science and Technology Organisation, Locked Bag 2001, Kirrawee DC, New South Wales, 2232, Australia*
[6]*SUPA, School of Physics and Centre for Science at Extreme Conditions, University of Edinburgh, Edinburgh EH9 3JZ, United Kingdom*
[7]*Center for High Pressure Science & Technology Advanced Research (HPSTAR), Shanghai 201203, People's Republic of China*
[8]*School of Physics and Astronomy, Queen Mary University of London, London E1 4NS, United Kingdom*
[9]*Institute for High Pressure Physics, RAS, 108440 Troitsk, Moscow, Russia*
[10]*Photon Science Institute and School of Electrical and Electronic Engineering, The University of Manchester, Oxford Road,*
Manchester M13 9PL, United Kingdom

We report experimental evidence for a crossover between a liquidlike state and a gaslike state in fluid methane (CH₄). This crossover is observed in all of our experiments, up to a temperature of 397 K, 2.1 times the critical temperature of methane. The crossover has been characterized with both Raman spectroscopy and x-ray diffraction in a number of separate experiments, and confirmed to be reversible. We associate this crossover with the Frenkel line—a recently hypothesized crossover in dynamic properties of fluids extending to arbitrarily high pressure and temperature, dividing the phase diagram into separate regions where the fluid possesses liquidlike and gaslike properties. On the liquidlike side the Raman-active vibration increases in frequency linearly as pressure is increased, as expected due to the repulsive interaction between adjacent molecules. On the gaslike side this competes with the attractive van der Waals potential leading the vibration frequency to decrease as pressure is increased.

I. INTRODUCTION

For centuries, the existence of a first-order phase transition, involving a large discontinuous change in density, between the liquid and gas states of matter, has been understood. Applying high pressure shifts this transition to higher temperatures. In 1822 the critical point was discovered [1], a specific pressure (P_c) and temperature (T_c) where the first-order phase transition line between liquid and gas states ends. Beyond this point, a discontinuous change in a physical observable distinguishing between a liquidlike and gaslike state in the sample cannot be discerned. Matter in this *P-T* region is therefore described as a "supercritical fluid," neither a liquid nor a gas.

Theoretical description of the liquid and supercritical fluid phases has been a challenge ever since. Previously the common approach was to treat liquids and supercritical fluids as dense nonideal gases [2], justified on the basis that liquids and supercritical fluids share important properties with gases, for instance, a lack of long-range order. A path on a *P-T* phase diagram can commence in the gas phase, pass above the critical point, and end in the liquid phase without encountering a first-order phase transition. While no discontinuous change in a physical observable can be observed beyond the critical point, the understanding of the supercritical fluid phase as a dense nonideal gas has led to the prediction, and observation, of some other crossovers extending a finite distance from the critical point.

There are, firstly, a group of crossover lines emanating from the exact critical point and extending to higher temperatures and pressures called the Widom lines. The Widom lines are maxima in certain thermophysical properties such as the speed of sound, and isochoric and isobaric heat capacities. Further away from the critical point the maxima become more smeared out and the different Widom lines diverge from each other [3–5]. No Widom lines are expected to exist beyond $T/T_c \approx$ 2.5 and $P/P_c \approx 3$ [2].

Also beginning in the vicinity of the critical point (but not necessarily emanating from the exact critical point) are the Joule-Thomson inversion curve and Boyle curve. At temperatures up to ca. $3T_c$ lines of constant enthalpy can be traced across the *P-T* phase diagram. Each line, as pressure is varied, reaches a maximum temperature. These maxima are linked by the Joule-Thomson inversion curve [6,7]. In a similar manner, the Boyle curve and (at higher pressure) the Amagat curve can be traced out. The nature of these lines is highly relevant to the industrial applications of supercritical fluids, for instance, the use of the Joule-Thomson effect in refrigeration technology.

However, as pressure is increased the density of a liquid (or supercritical fluid) becomes close to that of a solid, orders of magnitude larger than the density of a gas. The latent heat of vaporization is usually an order of magnitude larger than the latent heat of fusion, and liquids (unlike gases) can exhibit orientational order similarly to solids. Therefore,

---

*Corresponding author: j.e.proctor@salford.ac.uk

instead of treating liquids as dense nonideal gases, the opposite theoretical approach has also been utilized—treating them similarly to solids, assuming (relatively) closely packed atoms [8–10]. This approach was first put forward by Frenkel in several publications leading to *Kinetic Theory of Liquids* [8] and also by Lennard-Jones and Devonshire [11,12]. In this approach, the molecules (or atoms in an atomic liquid) have definite positions, with occasional vacancies [8,13], which can be treated in a manner similar to vacancies in solids. This is necessary to understand the heat capacities of liquids [10] and to understand why, unlike gases, liquids do support high-frequency shear waves [14].

A key element of Frenkel's theory is the introduction of the liquid relaxation time τ_r. Frenkel proposed that, on short time scales, the molecules in a liquid exhibit only vibrational motion around an equilibrium position, similar to that in a solid. However, the molecules occasionally jump to a new equilibrium position by swapping places with an adjacent molecule or vacancy. The liquid relaxation time τ_r is the average time that a molecule spends in a certain equilibrium position, between consecutive jumps. On time scales shorter than this, Frenkel proposed, the liquid could support shear waves just like a solid. This ability to support shear waves, with period shorter than the liquid relaxation time τ_r, has been verified experimentally [14] and has allowed accurate prediction of the heat capacities of liquids [10].

Shear waves can therefore be supported in liquids with periods ranging from a minimum of the Debye vibrational period τ_0 up to a maximum of τ_r. The Debye period τ_0 does not change significantly with temperature but τ_r is expected to decrease by orders of magnitude as temperature increases due to the greater amount of thermal energy available [15]. Therefore, under an isobaric temperature increase commencing in the liquid region (at higher pressure and lower temperature than the critical point), a point is eventually reached where due to the decrease in τ_r no shear wave can be supported since $\tau_r < \tau_0$. Thus there is a crossover here from liquidlike to gaslike behavior, which has been named the "Frenkel line" [15].

The Frenkel line is a different phenomenon from the Widom lines [3]. We predict (for instance, in CO_2, H_2O, CH_4 [16], and Ne [17]) that the Frenkel line at T_c lies at substantially higher pressure than P_c, where the Widom lines begin. In CH_4 $P_c = 4.5$ MPa, while the Frenkel line at T_c is predicted to occur at 54 MPa [16]. This is because, as Frenkel pointed out [8], the fluid density close to the critical point is far too low for the solidlike description of the liquid as a relatively close packed arrangement of molecules to be valid. As temperature is increased, both the Widom lines and the Frenkel line are crossed at higher pressure but roughly the same density. Thus, at a given temperature, the Frenkel line is always crossed at significantly higher pressure and density than the Widom lines. Furthermore, the Widom lines extend a finite distance from the critical point [3,4] while the Frenkel line is expected to extend to arbitrarily high *P-T*.

The liquidlike or gaslike environment affects the vibrations of individual molecules. Many vibrations are measurable using Raman or infrared spectroscopy and this gives insight into the environment as vibrational frequencies depend on both the density and dynamics of the sample. In a liquid as described

by Frenkel, the frequency of vibrations detectable using Raman and infrared spectroscopy should increase in a linear or slightly sublinear manner, upon pressure increase, similarly to a solid. This is understood by considering a solid described by the simplest equation of state (EOS), the Murnaghan equation [18,19]:

$$\frac{V(P)}{V_0} = \left[1 + \frac{K_0'P}{K_0}\right]^{-\frac{1}{K_0'}}. \tag{1}$$

Here, K_0 is the bulk modulus and K_0' its pressure derivative. Provided the application of pressure does not substantially modify the nature of the interatomic bonds, one can also relate the sample volume to vibrational frequency $\omega(P)$ using a positive constant Grüneisen parameter γ for that mode [20]:

$$\frac{\omega(P)}{\omega_0} = \left[\frac{V(P)}{V_0}\right]^{-\gamma}. \tag{2}$$

We can hence predict the variation of $\omega(P)$ with pressure:

$$\frac{\omega(P)}{\omega_0} = \left[1 + \frac{K_0'P}{K_0}\right]^{\frac{\gamma}{K_0'}}. \tag{3}$$

Generally, $K_0' \approx 4$ (it is frequently fixed at 4.0 [19]), and for typical Raman-active vibrational modes $\gamma \approx 2 - 4$. Hence $\omega(P)$ increases in a linear or slightly sublinear manner upon pressure increase. This is almost always observed in dense liquids, and amorphous and crystalline solids due to the interaction between adjacent atoms being entirely repulsive under pressure [Eq. (2) is a consequence of this].

Conversely, in a gas—and in the *P-T* region that we will propose here as the gaslike side of the Frenkel line—there is competition between the repulsive potential and attractive van der Waals forces between adjacent molecules undergoing ballistic motion. Attractive van der Waals forces dominate in a gas at the lowest pressures and lead the vibrational frequencies to decrease upon pressure increase [21]. Thus, the variation of vibrational frequencies as a function of pressure in an isothermal experiment can display a minimum as one proceeds from the gaslike side to the liquidlike side across the Frenkel line, and can be described by a quadratic or cubic function rather than a linear or slightly sublinear function [22,23].

Experimentally, a number of spectroscopy studies have been conducted on gases and supercritical fluids at very low pressure up to ca. 500 bars [21,24–26], observing the decrease in vibrational frequencies upon pressure increase. In a few cases these studies have reached a pressure where there is a minimum in the vibrational frequency as the repulsive interatomic forces begin to take effect [24], but none have reached the regime on what we now propose as the liquidlike side of the Frenkel line, where repulsion completely dominates over the van der Waals forces.

Additionally, many spectroscopy studies have focused on solids and dense liqusids in the diamond anvil cell (DAC) to characterize the nearly linear increase in vibrational frequencies as a function of pressure in these *P-T* regions [27–29]. However, the low-pressure region where the repulsive part of the interatomic potential competes with attractive van der Waals forces has not been characterized in such studies. This is partially because it is challenging to control and measure pressure in the DAC with sufficient accuracy to study this

region, and perhaps also because the scientific importance of this region has not been widely recognized.

We have utilized both spectroscopy and diffraction to probe the EOS, and structural and dynamic nature of supercritical fluid CH_4 from ambient pressure up to the melting curve, from 298 to 397 K. We present a unified set of data covering both the low-pressure regime (in which the repulsive interatomic potential competes with attractive van der Waals forces) and the high-pressure regime (in which the repulsive interatomic potential dominates). The Widom lines are not expected to exist beyond $T/T_c \approx 2.5$ and $P/P_c \approx 3.0$ [15]. As CH_4 has T_c of 190 K and P_c of 4.6 MPa [30], our investigations probe pressures beyond where the Widom lines for CH_4 are expected to lie and at pressures which are applicable to the interiors of the gas giants Uranus and Neptune which are rich in CH_4.

II. EXPERIMENTAL AND ANALYSIS METHODS

Donut (for experiments at ambient temperature) and piston-cylinder (for experiments at high temperature) diamond anvil cells (DACs) were constructed in house. The DACs were equipped with diamonds having 600- and 450-μm-diameter culets, and stainless steel gaskets. CH_4 was liquefied inside a cryogenic loading apparatus by cooling the apparatus with liquid N_2. The DACs were then closed while completely immersed in liquid CH_4. The liquid N_2 does not enter the cryogenic loading apparatus during this procedure, and the strong Raman-active N_2 vibration was not observed at any point during our experiments.

To perform the high-temperature experiments, the DACs were heated using a resistive heater surrounding the entire DAC (Watlow Inc.) and temperature was controlled with a precision of ± 2 K using a custom-constructed temperature controller. Temperature was measured using K-type thermocouples in contact with the diamond or gasket.

Pressure was measured at ambient temperature using the ruby photoluminescence method, resulting in a typical error of ± 0.002 GPa. In all cases error bars are too small to display. At temperature above 300 K pressure was measured using the Sm:YAG photoluminescence method using the $Y1$ peak [31], and was measured before and after the collection of each data point due to the greater risk of pressure fluctuation at high temperature. The typical error in each individual pressure measurement is ± 0.003 GPa; however, some pressure fluctuation occurred while the CH_4 Raman spectra were being collected. The error bars displayed in Fig. 3 are the result of this fluctuation. Except where otherwise stated, data were collected on pressure decrease at constant temperature.

X-ray diffraction patterns from fluid CH_4 were collected on beamline ID27 at the European Synchrotron Radiation Facility. The beam size was 3 μm × 2 μm and Soller slits were utilized to reduce the background signal coming from the diamond anvils. The background (a diffraction pattern collected from the empty DAC) was subtracted from each integrated pattern after normalization in the high-q limit (Fig. 1).

Raman spectroscopy was performed using 532-nm laser excitation, backscattering geometry, and a conventional single grating (1200 lines per inch) Raman spectrometer. The spectrometer was calibrated using the Raman peaks from silicon and diamond collected at ambient conditions. After
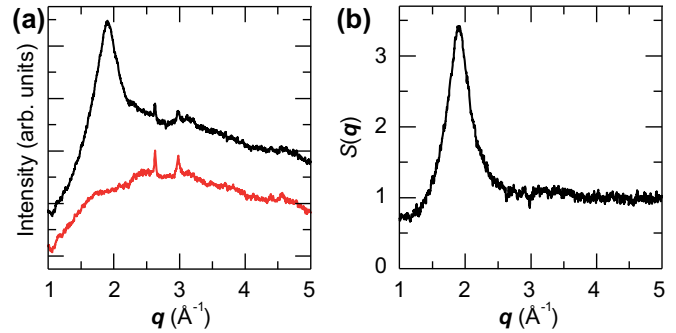

FIG. 1. Background correction of integrated diffraction patterns. (a) Diffraction pattern of fluid CH_4 at 0.69 GPa (black, upper) and background from empty DAC (red, lower). (b) Static structure factor $S(q)$ of CH_4 at 0.69 GPa obtained by subtracting background and normalizing in the high-q limit.

background subtraction, the strong Raman peak from the v_1 symmetric stretching vibration of CH_4 at ca. 3000 cm^{-1} was fitted with a single Lorentzian curve, allowing the determination of the peak positions with a typical accuracy of ± 0.05 cm^{-1}. In all cases the error bars are too small to display. Our investigation was carried out at pressures where we would not expect to observe any rotational substructure to the peak.

All Raman spectra were collected using 180° backscattering geometry through the cylinder diamond. To ensure the greatest accuracy possible in our measurements of the intensity of the v_1 peak we focused on the same point on the diamond culet before collecting each Raman spectrum. The second-order Raman band from the diamond (between 2500 and 2700 cm^{-1}) was collected in the same Raman spectrum as the v_1 methane peak and the drastic changes in intensity of the v_1 discussed later were clearly observed relative to the intensity of the second-order diamond band intensity remaining constant.

III. RESULTS AND DISCUSSION

We collected x-ray diffraction patterns of fluid CH_4 at 298 K. We observed the first peak in the fluid CH_4 structure factor $S(q)$ with reasonable intensity (Fig. 1), used its position to derive the volume occupied by the CH_4 molecule, and plotted the EOS of fluid CH_4 from very close to ambient pressure, up to the melting point at 1.35 GPa [32] [Fig. 2(a)]. The data are fitted with a Murnaghan EOS [Eq. (1)], and with an ideal gas EOS with van der Waals correction [13] [Eq. (4), where A, B, and C are constants].

$$V(P) = \frac{A}{P - C} - B. \tag{4}$$

Both equations provide a good fit to the data. However, it is important to note that these data do not provide an accurate measure of the density. This is because, to obtain the density from the volume occupied by a single molecule, one needs to assume a certain coordination number, packing arrangement, and concentration of holes in the fluid. These factors are unknown.

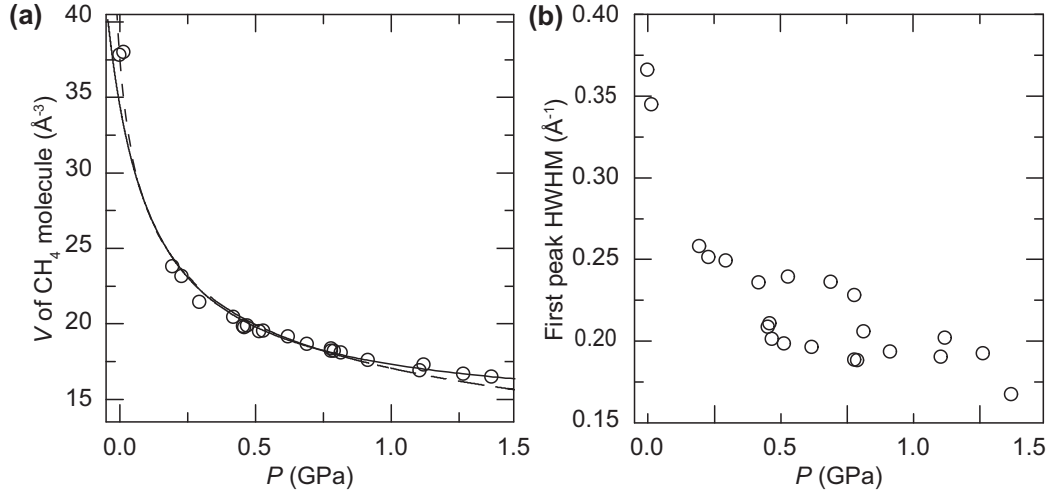We also plot [Fig. 2(b)] the width [half width at half maximum (HWHM)] of the first peak in $S(q)$. This increases

FIG. 2. (a) Equation of state (EOS) of fluid CH_4 at 298 K. Circles: experimental data. Solid line: Fit of ideal gas EOS modified with van der Waals correction [Eq. (4)]. Dotted line: Fit of Murnaghan EOS [Eq. (1)]. (b) HWHM of first peak in $S(\boldsymbol{q})$ plotted as a function of pressure at 298 K.

significantly at extremely low pressures, consistent with the sample being in a gaslike state instead of a liquidlike state [8,13]. However, in contrast to a recent report on supercritical Ar [33], we observe no evidence for a discontinuity in the position (Fig. S1 in the Supplemental Material [34]) or width [Fig. 2(b)] of $S(\boldsymbol{q})$ as a function of pressure. Such a discontinuity is not expected, since it is determined by the density which varies smoothly this far beyond the critical point [13,17,30].

We attribute the large scatter in x-ray diffraction data points (especially the width) to relatively weak scattering from the sample and errors introduced during the background subtraction procedure.

However, using Raman spectroscopy we observe much clearer evidence for a crossover. Figure 3 shows the reduced frequency of the Raman-active υ_1 vibration of CH_4 upon pressure increase at 298, 345, 374, and 397 K. In all cases, at higher pressure the shift in vibration frequency upon pressure increase is positive and linear, as expected from a dense liquid. At lower pressure, the vibration frequency decreases slightly upon pressure increase before reaching a minimum and increasing as the higher-pressure region is reached. The observed trend in peak position is reversible with no hysteresis within experimental error (see the Supplemental Material [34] for additional plots and clarifications).

Therefore, we propose that in the high-pressure region the vibration frequency is described by Eq. (2)—i.e., its pressure-induced shift is entirely due to the repulsive interaction between CH_4 molecules—and make linear fits to the data above 0.6 GPa [using Eq. (5), where c_1 and c_2 are constants]. This provides a good fit to the data above 0.6 GPa at all temperatures studied (298, 345, 374, and 397 K) and c_2 remains constant (within error) at $0.004\,\mathrm{GPa}^{-1}$. The value of ω_0 was fixed at the observed vibration frequency for the lowest-pressure data point at each temperature (in all cases lower than 0.1 GPa).

$$\frac{\omega(P)}{\omega_0} = c_1 + c_2 P. \qquad (5)$$

However, in the low-pressure region the repulsive potential [responsible for the increase in Raman frequency, Eqs. (3) and (5)] competes with the attractive van der Waals interaction between CH_4 molecules, which causes a decrease in Raman frequency as pressure is increased. Since the attractive van der Waals contribution becomes weaker as pressure is increased we describe it using an exponential decay function. The total Raman shift as a function of pressure is therefore given as follows:

$$\frac{\omega(P)}{\omega_0} = c_1 + c_2 P + (1 - c_1)e^{-c_3 P}. \qquad (6)$$

Here, c_1 and c_2 are the constants which remain fixed following our fits to the data above 0.6 GPa while c_3 is adjusted so that Eq. (6) provides the best fit to the entire data set. To evaluate when liquidlike behavior becomes dominant over gaslike behavior, we obtain the pressure at the minimum in the fit to the graph of $\frac{\omega(P)}{\omega_0}$. It is clear from Fig. 3 that due to the spread of data and lack of Raman data points at extremely low pressure this curve fit is not always well constrained.

For comparison we therefore examined our data using two other methods. We fitted straight lines to the data points lying on each side of the perceived "kink" in the graph of reduced Raman frequency (Fig. 3) and calculated the crossover pressures as where these lines intersect, as performed in the previous diffraction studies reported in Refs. [33] and [35]. This shifts our crossover pressures higher, especially at 397 K (see the Supplemental Material [34]). This procedure, in contrast to the fit using Eq. (6), is purely phenomenological. It assumes a completely discontinuous transition (none of the proposed transitions or crossovers in the supercritical fluid regime are expected to be completely discontinuous) and it involves some preconception of where the "kink" and therefore crossover pressure lies. In the fit using Eq. (6) there is no assumption as to where the crossover lies, or even that it exists at all—there is nothing in the curve fitting procedure to prevent c_3 converging to a small value or zero. This did not happen.

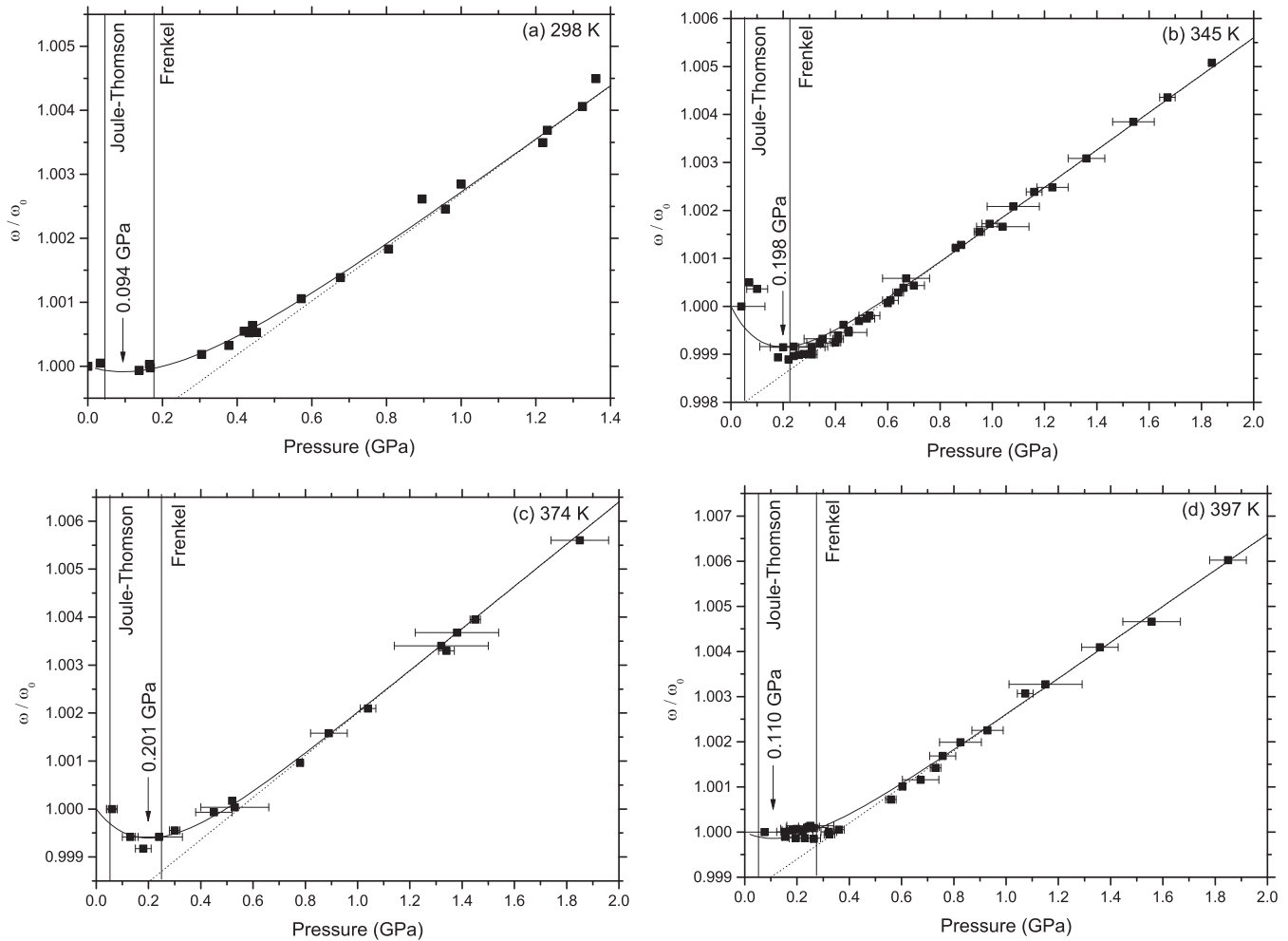We have also plotted in Fig. 3 the theoretically expected positions of the Joule-Thomson curve and Frenkel line in CH_4,

FIG. 3. Plot of reduced frequency of CH_4 Raman-active vibration as a function of pressure at (a) 298 K, (b) 345 K, (c) 374 K, and (d) 397 K. Solid lines following the data are fits performed using Eq. (6) and arrows signify the minimum of this fit. Dotted lines are linear fits to data collected above 0.6 GPa [Eq. (5)]. Vertical solid lines are expected positions of the Joule-Thomson line and Frenkel line.

for direct comparison to our actual Raman data points (see later discussion).

Since the procedure of using only linear fits is purely phenomenological and the direct comparison of our data points to theoretically predicted crossovers does not produce a numerical value for the experimentally observed crossover we use Eq. (6) for our determinations of the crossover pressure. While the curve fits are poorly constrained in this study, the procedure can provide a framework for future investigations. These fits at all temperatures studied are shown in Fig. 3.

We observe an additional phenomenon at pressure close to the minimum in each case, a discontinuous change in the integrated intensity and width of the Raman peak. Figure 4(a) shows this at 298 K. This change in intensity, peak position, and width is also reversible at all temperatures studied (see the Supplemental Material [34]). It remains unclear exactly how the transition from the liquidlike to gaslike behavior causes this phenomenon; however, we can see possible links. For instance, the propagation of shear waves on the liquidlike side of the Frenkel line could cause localized compression of some areas of the fluid with a resulting broadening of the Raman peak.

In Fig. 5 we plot the crossover pressures found using the procedure above [Eq. (6)], at all temperatures studied. The crossover shifts to higher pressure as temperature is increased as expected, but we note the significant scatter in the data due to the poorly constrained curve fits using Eq. (6). While the crossover pressure obtained at 397 K using Eq. (6) is somewhat lower than that at 374 K, the alternate methodology of fitting straight lines to the data above and below the perceived "kink" in each data set results in a crossover pressure of 0.36 GPa at 397 K (see the Supplemental Material [34]).

The given errors in crossover pressures in Fig. 5 are calculated from the errors on the fitted parameters c_2 and c_3 in Eq. (6). However, we expect the real error in these pressures is slightly larger. This is due to the method of pressure measurement, photoluminescence from a Sm:YAG crystal in the sample chamber. At high temperature, the photoluminescence peak used to measure pressure broadens and merges with the neighboring peak (see example spectra in the Supplemental Material, Fig. S7 [34]). This produces an error in pressure measurement which is hard to quantify, and is what limited the temperature achievable in this study. We recommend the development of pressure sensors providing
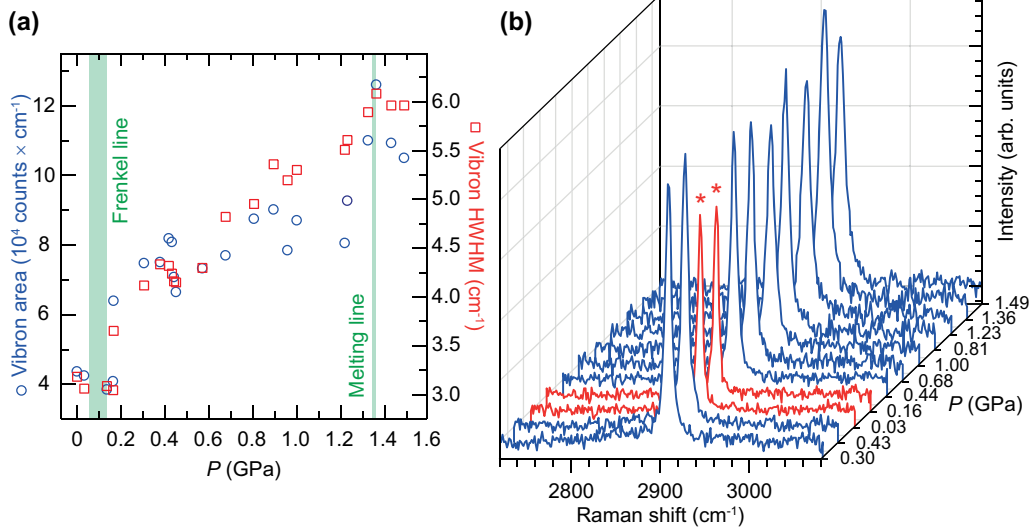
FIG. 4. (a) Plot of Raman peak area (integrated intensity, blue circles) and HWHM (red squares) as a function of pressure at 298 K, showing discontinuous decrease in both area and HWHM when the gaslike side of the Frenkel line is reached. The green shaded region is the area in which the minimum in vibration frequency [fitted using Eq. (6)] lies, which we associate with the Frenkel line and the green line marks the experimentally measured melting line [32]. (b) Waterfall plot of spectra collected at 298 K in order collected, demonstrating the reversible nature of the crossover. Red spectra (marked with asterisks) are those on the gaslike side of the Frenkel line.

more accurate pressure measurement above 400 K at modest pressures, to address this problem.

Despite limitations imposed by the need for accurate pressure measurement, we have succeeded in observing a crossover in CH_4 at $44P_c$ using Eq. (6) ($77P_c$ using the alternate fitting methodology outlined in the Supplemental Material [34]) and $2.1T_c$. The Widom lines are not expected to persist up to this pressure and we have confirmed this for the Widom lines in CH_4 (see the Supplemental Material [34] and Ref. [30]).

We therefore compare our crossover pressures to the expected positions of the Boyle curve, Joule-Thomson curve,

and Amagat curve (calculated using the Wagner-Setzmann equation of state for methane and the THERMOC package [36]) and the expected position of the Frenkel line [16] [Fig. 5(b)]. Out of these options, only the Joule-Thomson curve and Frenkel line lie close enough to our observed crossover to be feasible candidates to explain it.

In terms of pressure, our crossover pressures (when obtained using Eq. (6) as shown in Fig. 5, or using linear fits as shown in the Supplemental Material [34]) lie, on average, closer to the Frenkel line than the Joule-Thomson curve. Alternatively, we could discuss the data in terms of density. Since, at higher pressure, a particular increase in pressure
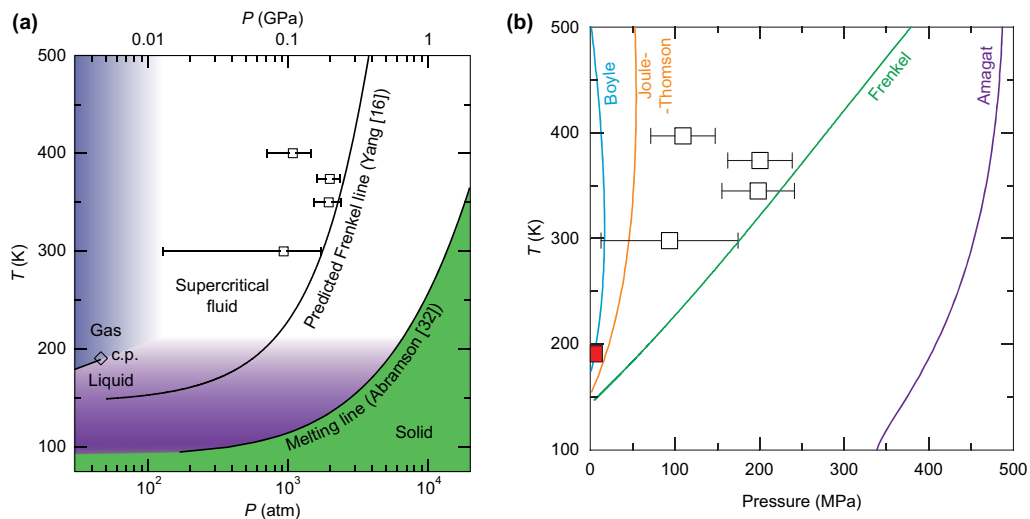

FIG. 5. Phase diagram of CH_4. (a) The theoretically predicted Frenkel line in CH_4 [16] is marked along with the experimentally observed melting curve [32]. The data points are the crossovers we observe experimentally and attribute to the Frenkel line. (b) The position of the theoretically predicted Frenkel line compared to the Boyle curve, Joule-Thomson curve, and Amagat curve. Open squares are our Frenkel line data points and the red closed square is the critical point (c.p.).

produces a smaller increase in density, this would shift our crossover pressures even closer to the Frenkel line than the Joule-Thomson curve. In terms of temperature, our crossovers lie at pressures where the Joule-Thomson curve is not predicted to exist, at any temperature.

A direct comparison of the expected positions of the Frenkel line and Joule-Thomson curve to our plots of Raman frequency against pressure (Fig. 3) reveals that the expected Frenkel line lies, at all temperatures measured, closer to the point where the Raman frequency stops decreasing upon pressure increase and starts increasing, than the Joule-Thomson curve.

The predicted Amagat curve lies at significantly higher pressure than the Frenkel line (over $3\times$ the pressure of the Frenkel line at 300 K). The prediction of the Amagat curve, just like that of the Boyle curve and Joule-Thomson curve, stems from an understanding of the supercritical fluid state as a dense nonideal gas. We argue, therefore, that the predicted Amagat curve is not meaningful on account of the fact that it lies at significantly higher pressure than the Frenkel line. In this P-T region we propose that the fluid must be treated as a solid in which the molecules are relatively closely packed with specific positions and only occasional vacancies.

We propose that the Frenkel line is the most plausible explanation for our observations, on account of the fact that it lies the closest to our data points, and because the behavior of the Raman-active vibration and first $S(\boldsymbol{q})$ peak on the low-pressure side of the crossover we observe are as expected for a gaslike sample while their behavior on the high-pressure side of the crossover are as expected for a liquidlike sample. This is the distinction that the Frenkel line makes. Furthermore, we observe (see Fig. 4) a discontinuous, reproducible, and reversible change in the intensity and width of the Raman peak at pressure close to the minimum in each case. There are plausible mechanisms by which this can be associated with the Frenkel line (for instance, the propagation of shear waves through the fluid on the liquidlike side could cause local variation in density and hence broadening), but we can see no mechanism by which the observed discontinuous change could be associated with the Joule-Thomson line.

IV. CONCLUSIONS

We have observed a narrow crossover between liquidlike and gaslike behavior in CH_4 at 400 K, $44 - 77 P_c$ (depending on the curve fitting method) and $2.1 T_c$. We propose the Frenkel line as the most likely explanation for this observation. The observation of this crossover in a simple molecular fluid has major implications for planetary science—in particular concerning Uranus, where the atmosphere is thought to be isolated from its interior, evidenced by anomalously low heat flow measurements from the Voyager spacecraft [37] and storm activity attributed to seasonal change in incident solar flux [38]. These findings have been attributed to the remnant heat

of Uranus being trapped beneath a less conductive layer [39]. We believe [10,15,40] that the thermal conductivity and other heat-related properties of fluids change significantly when the Frenkel line is crossed, and that this is likely to occur in the transition zone between the atmosphere and mantle of Uranus, and Neptune. Furthermore, understanding the Frenkel line in other dominant planetary species (hydrogen, helium, water, and ammonia) would improve our understanding of all gas giants. We believe the findings presented here will be relevant to characterization of supercritical fluid inclusions in rocks [24,41] and industrial use of supercritical fluids.

This work also calls for the liquid state to be reexamined. A region in P-T space exists [Fig. 5(a)] where a sample exists on the liquidlike side of the boiling curve (so it is a liquid in terms of static properties) but on the gaslike side of the Frenkel line (so it is a gas in terms of dynamic properties). This region warrants careful study using modern experimental techniques.

We must acknowledge the growing body of evidence demanding a change in our understanding of the supercritical fluid state, despite the issue attracting controversy [17,33]. In addition to our observation of the Frenkel line here, a crossover has been observed using molecular dynamics simulations in Ar at $T/T_c = 3.0$ and $P/P_c = 100$ (attributed to a Widom line [4], and alternatively to the Frenkel line [15]). A crossover was observed very recently in Ne at $P/P_c = 250$ and $T/T_c = 6.6$ [35] and attributed to the Frenkel line. These works have observed crossovers in static [35] and dynamic [4] structure factors corresponding to the Frenkel line, while here we observe a crossover using Raman spectroscopy. The Raman frequency, as discussed above, depends on both the density and dynamics of the fluid. It exhibits a sharp crossover in all our experiments, which we associate with the Frenkel line. We conclude that the experimental evidence demonstrating that the supercritical fluid state is not a single homogeneous state is now irrefutable.

[1] C. C. de la Tour, Ann. Chim. Phys. **21**, 127 (1822).

[2] J. P. Hansen and I. R. McDonald, *Theory of Simple Liquids* (Elsevier, Amsterdam, (2007).

[3] F. A. Gorelli, T. Bryk, M. Krisch, G. Ruocco, M. Santoro, and T. Scopigno, Sci. Rep. **3**, 1203 (2013).

[4] G. G. Simeoni *et al.*, Nat. Phys. **6**, 503 (2010).

[5] A. R. Imre, U. K. Deiters, T. Kraska, and I. Tiselj, Nucl. Eng. Des. **252**, 179 (2012).

[6] E. H. Brown, Bull. Intnl. Inst. Refrig., Paris, Annexe **1960-1961**, 169 (1960).

[7] F. Reif, *Fundamentals of Statistical and Thermal Physics* (McGraw-Hill, New York, 1965).

[8] Y. I. Frenkel, *Kinetic Theory of Liquids* (Dover Publications, New York, 1955).

[9] K. Trachenko, Phys. Rev. B **78**, 104201 (2008).

[10] D. Bolmatov, V. V. Brazhkin, and K. Trachenko, Sci. Rep. **2**, 421 (2012).

[11] J. E. Lennard-Jones and A. F. Devonshire, Proc. R. Soc. London, Ser. A **163**, 53 (1937).

[12] J. E. Lennard-Jones and A. F. Devonshire, Proc. R. Soc. London, Ser. A **165**, 1 (1938).

[13] D. Tabor, *Gases, Liquids and Solids* (Cambridge University Press, Cambridge, 1969).

[14] W. C. Pilgrim and C. J. Morkel, J. Phys.: Condens. Matter **18**, R585 (2006).

[15] V. V. Brazhkin, Yu. D. Fomin, A. G. Lyapin, V. N. Ryzhov, and K. Trachenko, Phys. Rev. E **85**, 031203 (2012).

[16] C. Yang, V. V. Brazhkin, M. T. Dove, and K. Trachenko, Phys. Rev. E **91**, 012112 (2015).

[17] V. V. Brazhkin and J. E. Proctor, arXiv:1608.06883.

[18] F. D. Murnaghan, Am. J. Math. **59**, 235 (1937).

[19] W. B. Holzapfel, in *High-Pressure Physics*, edited by J. S. Loveday (CRC Press, Boca Raton, FL, 2012).

[20] B. Weinstein and R. Zallen, in *Light Scattering in Solids IV*, edited by M. Cardona and G. Güntherodt (Springer, Berlin, 1984).

[21] L. Shang, I.-M. Chou, R. C. Burruss, R. Hu, and X. Bi, J. Raman Spectrosc. **45**, 696 (2014).

[22] E. J. Hutchinson and D. Ben-Amotz, J. Phys. Chem. B **102**, 3354 (1998).

[23] D. Ben-Amotz and D. R. Herschbach, J. Phys. Chem. **97**, 2295 (1993).

[24] J. Zhang, S. Qiao, W. Lu, Q. Hu, S. Chen, and Y. Liu, J. Geochem. Explor. **171**, 20 (2016).

[25] K.-I. Saitow, H. Nakayama, K. Ishii, and K. Nishikawa, J. Phys. Chem. A **108**, 5770 (2004).

[26] H. Nakayama, K.-I. Saitow, M. Sakashita, K. Ishii, and K. Nishikawa, Chem. Phys. Lett. **320**, 323 (2000).

[27] Y. H. Wu, S. Sasaki, and H. Shimizu, J. Raman Spectrosc. **26**, 963 (1995).

[28] M. Hanfland, H. Beister, and K. Syassen, Phys. Rev. B **39**, 12598 (1989).

[29] B. A. Weinstein and G. J. Piermarini, Phys. Rev. B **12**, 1172 (1975).

[30] http://webbook.nist.gov/cgi/cbook.cgi?ID=C74828&Mask=4.

[31] A. F. Goncharov, J. M. Zaug, J. C. Crowhurst, and E. Gregoryanz, J. Appl. Phys. **97**, 094917 (2005).

[32] E. H. Abramson, High Pressure Res. **31**, 549 (2011).

[33] D. Bolmatov, M. Zhernenkov, D. Zav'yalov, S. N. Tkachev, A. Cunsolo, and Y. Q. Cai, Sci. Rep. **5**, 15850 (2015).

[34] See Supplemental Material at http://link.aps.org/supplemental/10.1103/PhysRevE.96.052113 for additional plots of x-ray diffraction and Raman peak characteristics as a function of pressure, information on curve fitting methods employed, pressure measurement, and Widom lines in CH_4.

[35] C. Prescher, Y. D. Fomin, V. B. Prakapenka, J. Stefanski, K. Trachenko, and V. V. Brazhkin, Phys. Rev. B **95**, 134114 (2017).

[36] http://thermoc.uni-koeln.de/.

[37] J. C. Pearl, B. J. Conrath, R. A. Hanel, J. A. Pirraglia, and A. Coustenis, Icarus **84**, 12 (1990).

[38] I. de Pater, L. A. Sromovsky, P. M. Fry, H. B. Hammel, C. Baranec, and K. M. Sayanagi, Icarus **252**, 121 (2015).

[39] T. Guillot, Science **269**, 1697 (1995).

[40] D. Bolmatov, V. V. Brazhkin, and K. Trachenko, Nat. Commun. **4**, 2331 (2013).

[41] D. S. Kelley *et al.*, Science **307**, 1428 (2005).